Dalton Transactions

ROYAL SOCIETY OF CHEMISTRY

PAPER

View Article Online
View Journal | View Issue

Cite this: *Dalton Trans.*, 2025, **54**, 3704

A double-chain based metallomicellar catalyst for aerobic oxidative synthesis of benzimidazoles in water†‡

Pragyansmruti Sunani, Prabaharan Thiruvengetam and Dillip Kumar Chand *

The oxomolybdenum complexes **Mo1**, **Mo2** and **Mo3**, which share a common ONO donor ligand backbone but differ in their peripheral substituents, were explored to study their reactivity in organic transformations in water. The ligand backbones of **Mo1** and **Mo2** were covalently linked to a methyl group and a single hydrophobic *n*-hexadecyl chain *via* an ether linkage, respectively. The complex **Mo3** was found to possess two *n*-hexadecyl chains attached to the ligand backbone *via* a common amine-N. Complexes **Mo2** and **Mo3** formed metallomicelle when dispersed in water due to the surfactant presence in their structures, enabling them to uptake organic substrates. The catalytic potential of the complexes was evaluated for the oxidative coupling of benzylamine with 1,2-diaminobenzene to synthesize benzimidazole in neat water using open air as the sole oxidant. The double-chain surfactant-type catalyst **Mo3** displayed superior activity compared to the single-chain surfactant-type complex, **Mo2**. A wide variety of benzimidazoles were synthesized in good to excellent yields under environmentally benign conditions using **Mo3** as the catalyst. The practical utility of the process was validated through multi-gram scale-up reactions and recyclability experiments. A plausible mechanism was proposed based on several controlled experiments and literature support.

Received 9th December 2024,
Accepted 6th January 2025

DOI: 10.1039/d4dt03406f

rsc.li/dalton

Introduction

Surfactants are widely used as catalysts or as additives with suitable transition metal-based catalysts to promote organic transformations in water.[1–4] In a metallosurfactant, the surfactant is integrated with the metal catalyst as a single molecule, thus offering greater advantages for organic transformations.[5–13] Due to their amphiphilic behavior, metallosurfactants undergo spontaneous aggregation to form metallomicelle, which occurs above the critical micelle concentration (CMC). These metallomicelles enrich organic substrates within their hydrophobic core, bringing them closer to the catalytically active species.[14–17] This enhanced interaction between the substrate and catalytic center significantly accelerates reaction rates. Our research focuses on developing diverse metallomicellar systems and exploring their application in various organic transformations in water.[10–13]

In general, metallosurfactants are designed so that the ligand backbone is connected to a hydrophobic chain, either through electrostatic interactions[10–12,18] or covalent bonding.[13,19–22] Among these, covalently bonded metallomicellar systems have been proven to be more efficient catalysts compared to electrostatically linked systems, likely due to their enhanced catalytic stability and the fixed position of the metal units within the micellar aggregation.[13] The success of metallomicellar-catalyzed organic reactions in water depends not only on the catalyst center but also on the structure and aggregation behaviour of the metallosurfactants.

Oxomolybdenum complexes are well-explored as efficient catalysts for various oxidation reactions, however, they often involve harsh reaction conditions, hazardous oxidants, additives, and/or environmentally unfriendly organic solvents.[23–25] We have reported a non-surfactant-based molybdenum catalyst $MoO_2(\mathbf{L_1})(OH_2)$, **Mo1**, and a metallosurfactant, $MoO_2(\mathbf{L_2})(OH_2)$, **Mo2**, in which the ligand backbone is covalently bonded to one hydrophobic alkyl chain (Fig. 1). The metallosurfactant **Mo2** could efficiently catalyzed the oxidation of alcohols and lignin mimics into their corresponding carbonyls in a water medium, using open air as the oxidant.[13] We intended to prepare $MoO_2(\mathbf{L_3})(OH_2)$, **Mo3** (Fig. 1), with two alkyl chains connected to the ligand backbone, expecting higher activity,[21] and compare its reactivity with **Mo2** and **Mo1**.

Department of Chemistry, Indian Institute of Technology Madras, Chennai 600036, India. E-mail: dillip@zmail.iitm.ac.in

†Dedicated to Prof. Vadapalli Chandrasekhar on the occasion of his 65th birthday.

‡Electronic supplementary information (ESI) available: Synthesis and characterization of ligands, Mo-complexes, metallomicellar systems, catalysis protocols, reaction kinetics and characterization of catalytic products. See DOI: https://doi.org/10.1039/d4dt03406f

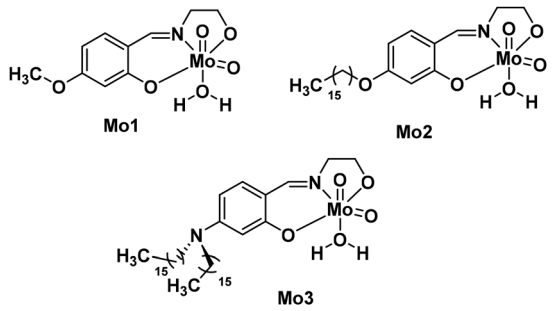

Fig. 1 Structures of oxomolybdenum complexes **Mo1**, **Mo2**, and **Mo3**.

Herein we report the synthesis of double-chain based catalyst **Mo3** and its use for oxidative coupling of benzylamine with 1,2-diaminobenzene to synthesize pharmaceutically important benzimidazoles[26–29] in water. The advantage of a double-chain catalyst over its single-chain complex, **Mo2**, under comparable conditions is also established in terms of lower reaction temperature and lower catalyst loading. The newly developed double-chain connected metallomicellar catalyst, **Mo3** produces the desired benzimidazoles in good yields under an aqueous environment, using open air as the sole oxidant, without involving any base/additives in contrast to the known methods that involve co-catalyst, additives, pressurized oxygen, and/or environmentally unfriendly organic solvents.[30–35] Our catalyst is found to be compatible with synthesizing a wide range of benzimidazoles comprising various functional groups. Further, the practical utility of the process is validated by performing multi-gram scale synthesis and reusability experiments of the catalyst.

Results and discussion

The catalyst

Synthesis of the molybdenum complex, **Mo3** is shown in Scheme 1. The precursors (**P$_3$**, **A$_3$**), Schiff base ligand (**L$_3$**(H)$_2$) and **Mo3** are all new compounds but they were synthesized using methods developed for related compounds. The precursor **P$_3$** was synthesized[36] using 3-aminophenol and 1-bromohexadecane as starting materials whereas **A$_3$** was synthesized by the Vilsmeier–Haack method.[37] The Schiff base ligand **L$_3$**(H)$_2$ was prepared by treating **A$_3$** with ethanolamine in methanol under reflux conditions for 3 hours.[38] The complex **Mo3** was prepared[13] by refluxing a mixture of the ligand **L$_3$**(H)$_2$ and $MoO_2(acac)_2$ in methanol for 3 hours followed by filtration to isolate a solid; the isolated solid was suspended in water and stirred for 1 hour to obtain the targeted complex. The obtained complex was thoroughly characterized by FT-IR, NMR spectroscopy, and ESI-MS spectrometry. The critical micellar concentration was determined using the conductivity method. The micellar aggregation behaviour in water was confirmed by high-resolution transmission electron microscopy (HR-TEM).

The presence of a single species in the solution was confirmed from ^{1}H and ^{13}C NMR of the complex recorded in $CDCl_3$ (ESI, Fig. S13 and S14‡). The ^{1}H NMR shows significant changes in chemical shift values for the complex **Mo3** compared to those for the free ligand. The complex was further characterized by FT-IR spectroscopy. Two strong bands in the region of 897 and 931 cm^{-1} can be assigned as symmetric and asymmetric stretching frequencies, respectively, due to *cis*-dioxo moieties (*cis*-MoO_2).[39] The hydrogen-bonded OH present in the free ligand shows a stretching frequency near 2700 cm^{-1}, which is absent in the spectrum recorded for complex **Mo3**. The presence of Mo–O bond with organic ligand was confirmed from the peaks appearing in the region of 636 cm^{-1}.[39] The bands at 1604 and 1523 cm^{-1} are assigned to the stretching frequency of C=N and C–O functional groups (ESI, Fig. S16‡). The ESI-MS data of the complex was recorded in positive ion mode in chloroform solvent. The segment containing molybdenum provides the isotopic pattern that corresponds to the mononuclear complex. The isotopic peak pattern (m/z = 757.4768) matched well with the simulated pattern (m/z = 757.4786) (Fig. 2). The crystallization of **Mo3** was tried, however, a suitable crystal was not obtained for mounting. Hence, the energy-minimized structures of **Mo3** are provided in lieu of the crystal structure (ESI, Fig. S17‡).

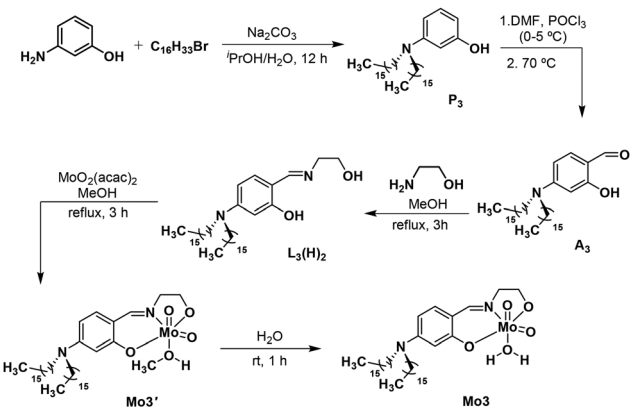

Scheme 1 Synthesis of the double-chain based oxomolybdenum complex **Mo3**.

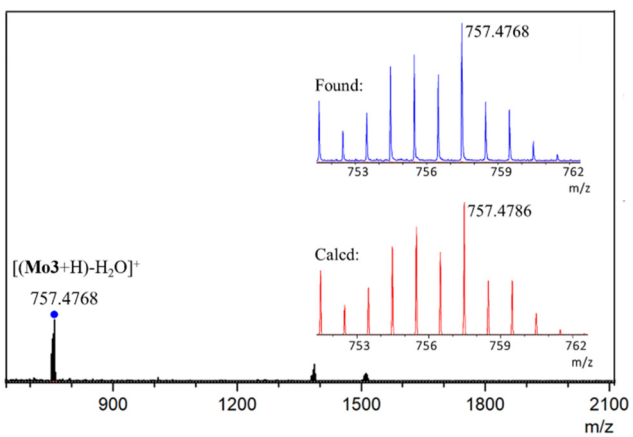

Fig. 2 Partial ESI-MS spectrum of complex **Mo3** in chloroform.

The critical micelle concentration (CMC) of the metallosurfactant, **Mo3** was determined from the conductivity measurement method and found to be 0.625 mM. It was observed that the double chain-based complex **Mo3** self-assembled to form aggregates in lower concentration compared to the single chain molybdenum complex, **Mo2**, whose CMC was determined to be 0.996 mM (Fig. 3). The micellar aggregation of the complex **Mo3** above CMC was further confirmed by HR-TEM analysis (Fig. 4).

Scope of the catalyst

After successful preparation and characterization of the metallomicellar complex **Mo3**, we intended to study the effect of double chain over single chain in reactivity of an organic transformation under comparable reaction conditions. In this regard, oxidative coupling of benzylamine with 1,2-diaminobenzene to generate 2-substituted benzimidazole in a water medium was chosen as the model reaction. The reaction was chosen with the purpose of delivering an efficient, cost-effective, and environmentally friendly route to synthesize N-heterocyclic compounds such as benzimidazoles from primary amine, unlike the reported methods that largely rely on the organic solvents for the required transformation.[30–35]

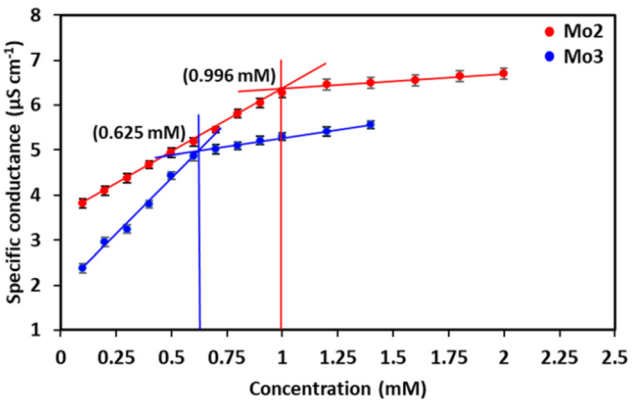

Fig. 3 Determination of critical micelle concentration (CMC) of **Mo2** and **Mo3**.

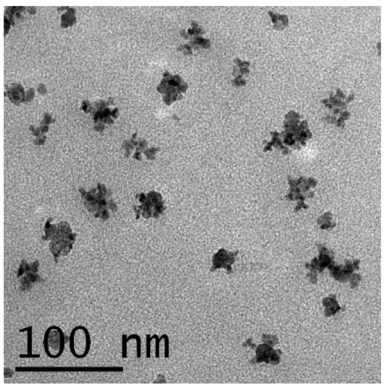

Fig. 4 HR-TEM image of metallomicellar complex **Mo3**.

The reaction conditions for the targeted organic reaction were optimized by taking benzylamine, **1a** and 1,2-diaminobenzene, **1b** as model substrates, varying the catalysts, catalyst loading, oxidant, temperature, and time. The acquired results are summarized in Table S1 (ESI‡).

We began our investigation by treating a slight excess of benzylamine, **1a** (0.9 mmol) with 1,2-diaminobenzene, **1b** (0.75 mmol) in 0.5 mL water, in the absence of a catalyst, at room temperature for 24 hours, under open air conditions. No product formation was observed (Table S1,‡ entry 1). However, when the reaction temperature was raised to 50 °C, a small amount of 2-phenyl-1*H*-benzimidazole, **1c** (<05% yield) was observed (Table S1,‡ entry 2). Based on this observation, we introduced 1.0 mol% of non-micellar catalyst, **Mo1**, to the reaction mixture, and heated it at 50 °C for 24 hours, resulting in a slight increment of the product yield to 11% (Table S1,‡ entry 3). Notably, the micellar catalysts with a single chain, **Mo2** (1.0 mol%), and double chain, **Mo3** (1.0 mol%) in the ligand backbone were employed under similar conditions, and the yield of **1c** increased significantly to 35% and 46%, respectively (Table S1,‡ entries 4 and 5). These results underscore the crucial role of the surfactant entity within the metal complex, which forms a metallomicelle during the reaction process, facilitating the reaction in a water medium. After proving the superior reactivity of the double chain-based catalyst, **Mo3**, over **Mo2** and non-micellar catalyst, **Mo1**, further optimization was conducted using **Mo3**.

To achieve a better yield of the desired product, the reaction temperature was increased to 80 °C, and **1c** was isolated in 83% yield (Table S1,‡ entry 6). A further increase in the reaction temperature to 100 °C did not result in a significant change in the product yield, where **1c** was isolated in 87% (Table S1,‡ entry 7). Notably, when the catalyst loading was increased to 1.5 mol% and the reaction was conducted at 80 °C for 24 hours, complete conversion was achieved, and product **1c** was isolated in 94% yield (Table S1,‡ entry 8). Reducing the reaction time to 18 and 12 hours led to isolated yields of 92 and 79%, respectively (Table S1,‡ entries 9 and 10). Thus, entry 9 in Table S1‡ is considered as the optimized reaction condition for the oxidative coupling of benzylamine, **1a** with 1,2-diaminobenzene, **1b** to form 2-substituted benzimidazole, **1c** catalyzed by **Mo3** (Scheme 2).

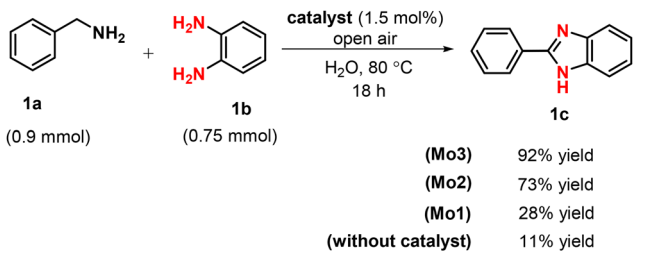

Scheme 2 Oxidative coupling of benzylamine, **1a** and 1,2-diaminobenzene, **1b** under optimized conditions using **Mo3**, **Mo2**, **Mo1** and in the absence of a catalyst.

Under these reaction conditions, the catalytic ability of **Mo2** was tested, resulting in only 73% of benzimidazole **1c** (Table S1,‡ entry 11). When the catalyst loading of **Mo2** was increased to 2.5 mol%, **1c** was isolated in 84% yield.

Only 28% and 11% yield of benzimidazole **1c** were isolated when the reactions were carried out using **Mo1** and in the absence of a catalyst under optimized reaction conditions (Scheme 2).

The effect of temperature on reaction progress using catalysts **Mo3** and **Mo2** was evaluated, by varying the reaction temperature while keeping other optimized conditions the same. The obtained results are plotted in Fig. 5. The yield of **1c** increased with the reaction temperature and complete conversion was observed at 80 °C using the catalyst **Mo3**, whereas **Mo2** requires a higher temperature (100 °C) for efficient conversion. Likewise, the effect of the catalyst concentration on the reaction rate was monitored using the more reactive catalyst **Mo3**. During the optimization of reaction conditions, the maximum yield of product **1c** was obtained when the catalyst concentration was maintained at 22.5 mM. Hence, keeping the optimized reaction conditions, the concentration of the catalyst was lowered up to 3.75 mM and the product formation was evaluated (Fig. 6). The observed results signify the efficient product formation at higher catalytic concentrations.

For further understanding, we performed the reaction kinetics for the oxidative coupling of benzylamine, **1a** with 1,2-diaminobenzene, **1b** to form benzimidazole, **1c** catalyzed by **Mo2** and **Mo3** under comparable reaction conditions. Conversion of 1,2-diaminobenzene, **1b** to benzimidazole **1c** was determined at specific time intervals by ^{1}H NMR spectroscopy using 1,3,5-trimethoxybenzene as the internal standard (Fig. 7a). The rates of the oxidative coupling reactions catalyzed by **Mo2** and **Mo3** were calculated from the $-\ln(1 - X_A)$ *vs.* time plot (Fig. 7b); the slope (k') values were obtained from the $-\ln(1 - X_A)$ *vs.* time graph and found to be 0.083 and 0.166 (h^{-1}), respectively. The second-order rate constants were calculated as 3.68 and 7.38 M^{-1} h^{-1} for **Mo2** and **Mo3**, respectively, indicating the high reactivity of double chain-based catalyst, **Mo3** compared to the single chain-based catalyst **Mo2** under standard conditions.

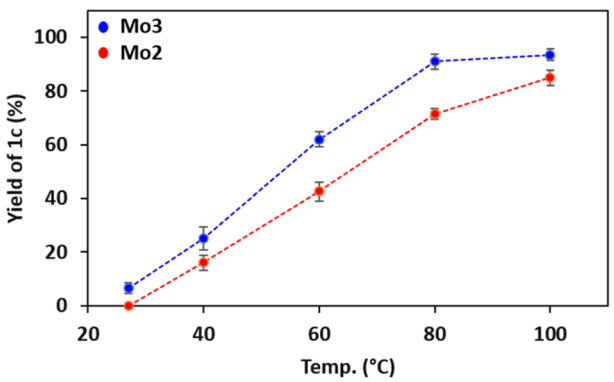

Fig. 5 Yield of **1c** catalyzed by **Mo3** and **Mo2** under optimized conditions as a function of temperature.

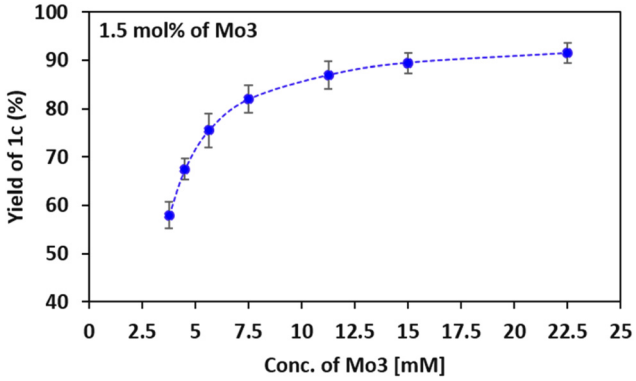

Fig. 6 Yield of **1c** under optimized conditions as a function of concentration of **Mo3**.

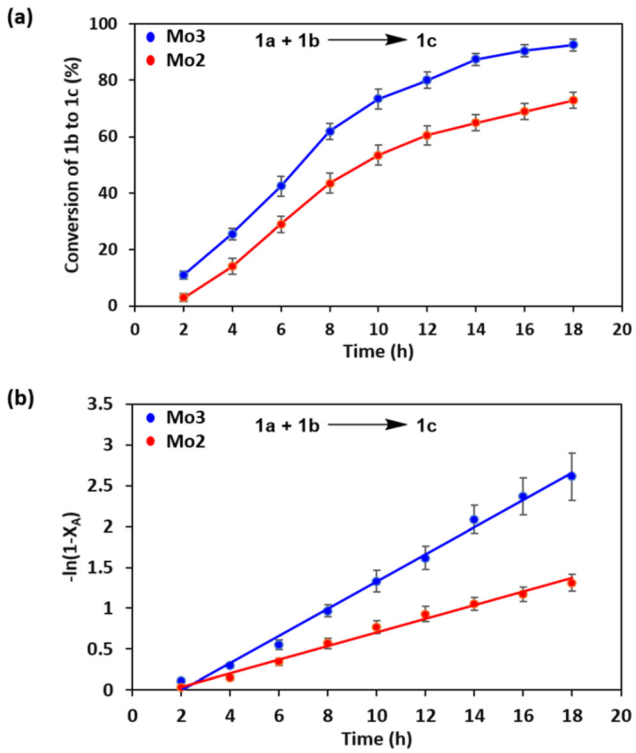

Fig. 7 **Mo2** and **Mo3** catalyzed (a) conversion of **1b** to **1c** at 2 h time intervals; (b) plot of $-\ln(1 - X_A)$ *vs.* time for the rate constant determination.

The efficient and environmentally friendly approach for the synthesis of benzimidazoles from benzylamine using a highly reactive and cost-effective catalyst **Mo3** inspired us to examine the versatility of the catalyst system towards a variety of substrates with different functional groups under the optimized reaction conditions and the results are summarized in Table 1. Interestingly, there is no apparent change in the product yield was observed despite the variations in the electronic nature of the benzene ring, indicating that the catalyst system operates effectively across a range of different substituents. Specifically,

Table 1 Synthesis of benzimidazole derivatives catalyzed by **Mo3** [a]

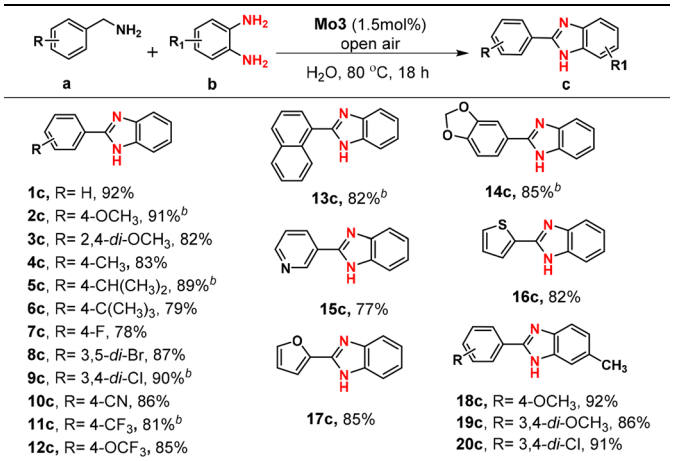

[a] Reaction conditions: benzylamines (0.9 mmol), 1,2-diamines (0.75 mmol) and **Mo3** (1.5 mol%) in 0.5 mL water at 80 °C (oil bath temperature) under open air. [b] The average yields are mentioned, and standard deviation in product yields range from ±1 to ±3.

benzylamines substituted with typical electron-donating groups such as methoxy, methyl, isopropyl, and *t*-butyl groups (**2a–6a**) were efficiently converted to the corresponding benzimidazoles with good to excellent yields (**2c–6c**). The methoxy groups substituted at *para* position (**2a**) provided better yield compared to the *ortho* position (**3a**). For benzylamine substituted with *t*-butyl group (**6a**), the yield of the corresponding benzimidazole (**7c**) was slightly lower at 79%. This decrease in the yield is likely attributed to steric hindrance caused by the bulky *t*-butyl group.

Likewise, benzylamine substituted with electron-withdrawing groups such as fluoro, bromo, chloro, cyano, and trifluoromethyl groups (**7a–11a**) underwent oxidative coupling with 1,2-diaminobenzene, **1b** and generated corresponding benzimidazoles in good yields (**7c–11c**). Benzylamines substituted with some other functional groups such as 4-trifluoromethoxy (**12a**), and naphthalen-1-ylmethanamine (**13a**) afforded corresponding benzimidazoles in good yields (**12c–13c**). The acetal group, a relatively weaker functionality, was tolerated during the reaction process and the corresponding benzimidazole **14c** was isolated in 86% yield. Further, hetero-atom-containing amines such as furfuryl amine (**15a**), 2-thiophene-methylamine (**16a**), and 3-pyridine methylamine (**17a**) were evaluated under the standard reaction conditions and moderate to good yields of benzimidazoles were obtained (**15c–17c**).

The catalytic activity of **Mo3** was also examined with methyl-substituted 1,2-diaminobenzene and reactions proceeded smoothly with a good yield of the desired products (**18c–20c**).

The excellent results from the substrate scope evaluation confirmed that the metallomicellar catalytic system is highly efficient in producing a wide range of benzimidazole derivatives with good to excellent yields in water using open air as the sole oxidant. This demonstrates the robustness, efficiency, and environmental sustainability of the catalyst system, as it operates under mild conditions without the need for external oxidants, making it a promising approach for green organic synthesis.

Gram-scale synthesis and recyclability experiments

To demonstrate the real-life applicability and synthetic validity of the current approach, gram-scale synthesis and recyclability experiments were performed under the optimized reaction conditions. We choose to synthesize 2-phenyl-1*H*-benzimidazole (**1c**) and a drug molecule, fuberidazole (**17c**) in a gram-scale for the scale-up reaction. In this line, 1.0 gram of benzylamine, **1a** was reacted with 0.84 gram of 1,2-diaminobenzene, **1b** with 1.5 mol% of the catalyst **Mo3** maintaining the optimal conditions, and 85% of benzimidazole, **1c** was obtained (Scheme 3a). Similarly, 1.0 and 2.0 grams of furfuryl amine, **17a** were subjected to 0.92 and 1.8 grams of 1,2-diaminobenzene, **1b** under standard conditions, and the desired product fuberidazole, **17c** was obtained in 80 and 73% yield, respectively (Scheme 3b). The lowered product yield during the gram-scale synthesis is likely due to potential mass transfer challenges caused by the slurry formation.

The catalyst recyclability experiment was performed to evaluate the long-term constancy of the catalyst. A series of reactions were kept taking benzylamine, **1a** (1.8 mmol) and 1,2-diamobenzene, **1b** (1.5 mmol) with 1.5 mol% of catalyst **Mo3** under optimized circumstances. The reusability and sustainability of the catalyst were examined by stopping the reaction after 18 h and using the same catalyst for the next run with the addition of fresh substrate. The organic compounds were separated from the aqueous layer by adding ethyl acetate to the reaction mixture. The organic layer was collected for the calculation of the yield of the desired product whereas the catalyst containing aqueous layer was used for the next cycle. The process was repeated for up to 8 cycles, and the yields were observed in the range of 92%–86% without any significant loss in the product yield (Scheme 4, blue color). The catalytic recyclability experiment was also performed under a kinetically controlled regime to evaluate the intrinsic ability of the catalyst throughout the reaction process. The reactions were stopped after 6 h and the organic compounds were extracted from the aqueous layer by phase separation adding ethyl acetate. The process was repeated for 8 cycles and the yield of

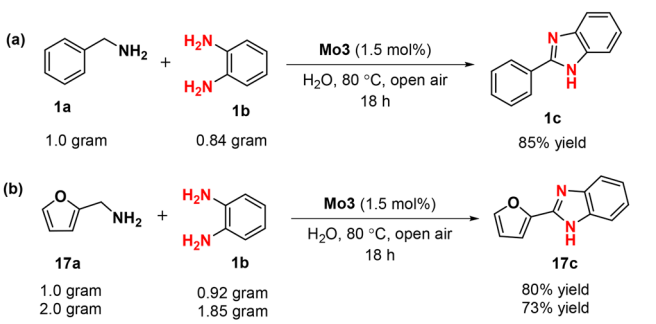

Scheme 3 Multi-gram scale synthesis of benzimidazole using **Mo3**.

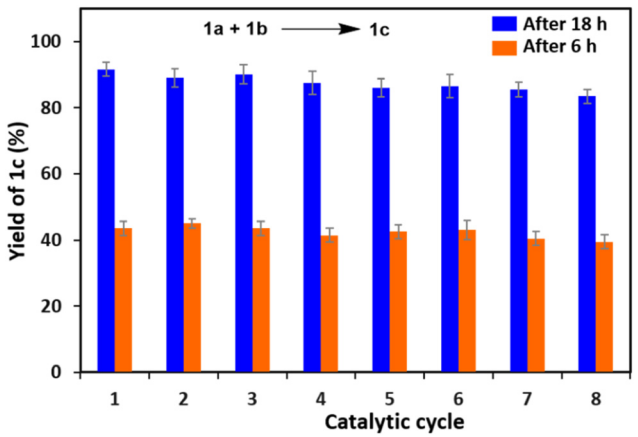

Scheme 4 Recyclability experiments of catalyst **Mo3**.

benzimidazole **1c** was isolated in the range of 46–41% (Scheme 4, orange color). These recyclability experiments prove the possibility of using the micellar catalyst **Mo3** for practical applications in a water medium under open-air conditions.

Benzaldehyde (oxidation product of excess benzylamine) was detected through a TLC experiment in the organic layer when the reaction was carried out for 18 h in a cycle. However, benzylamine (no benzaldehyde) could be detected when the reaction was stopped after 6 h. The presence of benzylamine in the water layer is inevitable in either case but such leftover benzylamine has no influence in the next cycle. This was confirmed by taking 1.5 equivalent of benzylamine in a separate experiment for synthesizing **1c** and found that the time taken and yields are not changed as compared to the use of 1.2 equivalents of benzylamine.

Reaction mechanism

On the basis of the experimental study and literature support, we proposed the plausible mechanism for the oxidative coupling of benzylamine and 1,2-diaminobenzene catalyzed by **Mo3**. In order to determine the reaction followed by ionic or radical pathway, a few controlled experiments were performed. In this line, catalyst **Mo3** was treated with 3 mol% of (2,2,6,6-tetramethylpiperidin-1-yl)oxyl (TEMPO) and 2,6-di-*tert*-butyl-4-methylphenol (BHT), both known as a radical inhibitor, under optimized reaction condition and no significant change in the yield of the product formation was observed (Scheme 5a and b). To obtain an insight into the mechanism and explore the formation of the oxoperoxo-molybdenum complex as the potential reaction intermediates, the catalyst **Mo3** was treated in water under molecular oxygen (through bladder) at 80 °C temperature and was stopped after 10 hours (Scheme 5c). The sample was analyzed by ESI-MS spectrometry and we were unsuccessful in locating any oxodiperoxo-molybdenum complex intermediate even after several trials. Based on the evidence and lack of support for a radical mechanism, an ionic mechanism was proposed instead of a radical pathway.

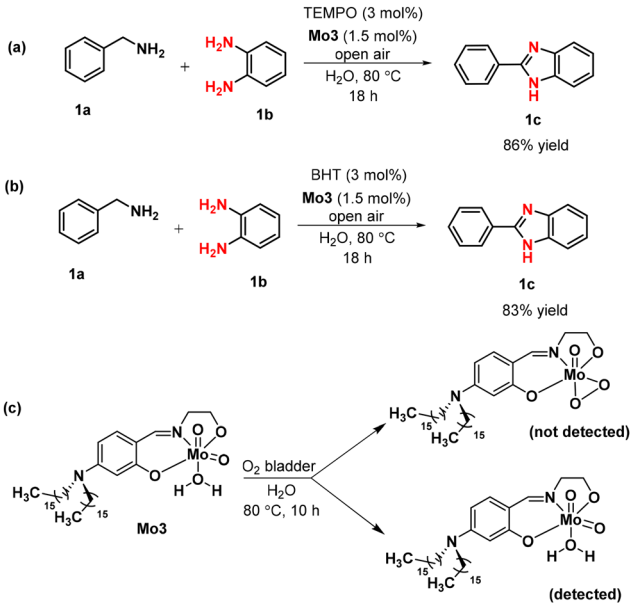

Scheme 5 (a) and (b) Oxidative coupling reactions in water catalyzed by **Mo3** in the presence of radical inhibitors; (c) trial conversion of molybdenum complex **Mo3** into peroxo complex (not feasible under employed conditions).

To determine the possible intermediates during the reaction for the formation of 2-substituted benzimidazole, a reaction was carried out in the absence of 1,2-diaminobenzene taking benzylamine as the starting material under standard conditions. We observed the complete conversion of benzylamine to benzaldehyde, **2a′** (Scheme 6a). However, when the reaction was carried out in a toluene medium (instead of H_2O) under standard conditions, it generated the homo-coupled aldimine product *N*-benzylidene-1-phenylmethanamine, **3a′** (Scheme 6b). It is proposed that **1a** is oxidized to phenylmethanimine, **1a′**, which reacted with another unit of **1a** to produce the homo-coupled product, **3a′**. However, in the presence of water at 80 °C, phenylmethanimine, **1a′** is hydrolysed to provide benzaldehyde, **2a′** in the absence of 1,2-diamine. During the reaction starting with benzylamine, **1a** and 1,2-dia-

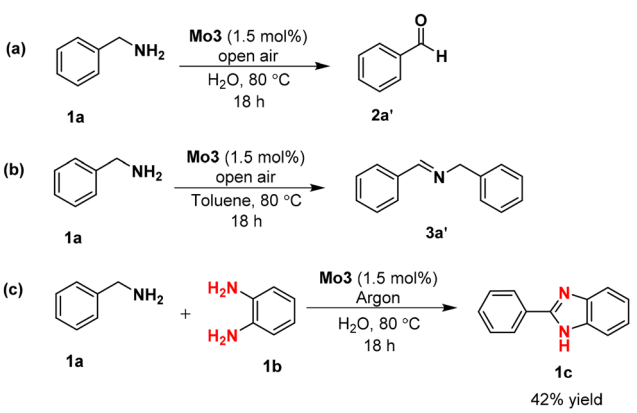

Scheme 6 Controlled experiments.

minobenzene, **1b** for synthesizing benzimidazole, aldehyde/imine was not traced. This signifies the generated imine from benzylamine immediately coupled with **1b** to provide the desired product **1c**. However, the complete or partial formation of aldehyde, **2a′** from imine, **1a′**, through hydrolysis with water at 80 °C cannot be entirely ruled out. To verify this, benzaldehyde, **2a′** was reacted with 1,2-diaminobenzene, **1b** and 1,2-disubstituted product, 1-benzyl-2-phenyl-1*H*-benzimidazole, **1c′** was found as a by-product, both, with or without the catalyst under optimized conditions. In contrast, the by-product **1c′** was not detected when the reaction started with benzylamine, **1a** and 1,2-diaminobenzene, **1b**. Hence, the slow production of imine from benzylamine using the catalyst **Mo3** helps in the selective formation of 2-substituted benzimidazole, **1c**. Further, to understand the role of oxygen, a separate reaction was carried out under an argon atmosphere and only 42% yield of **1c** was obtained, which clearly indicates that the reaction proceeded through aerobic oxidation where oxygen plays a crucial role in the high yield of the desired product (Scheme 6c).

To understand the fate of the catalyst **Mo3** during the catalysis reaction, we stopped the catalysed synthesis of **1c** after 10 h and separated the metal complex from the reaction mixture. The organic components were extracted from the aqueous reaction mixture using ethyl acetate. The metal-containing species were isolated by centrifugation of an aqueous layer and analysed by ^{1}H NMR, HRMS and FT-IR techniques. While the evidence for the existence of **Mo3** could be obtained, we do not have evidence to support the existence of metal–hydroxo species that are the likely intermediates.

Maeda *et al.* proposed a reaction mechanism for the oxidation of alcohol using an oxovanadium complex where the oxo–metal compound was converted to a hydroxo–metal intermediate.[40] From all the above experimental studies and literature reports, we propose an ionic pathway for the oxidation of benzylamine to respective imine, **1a′** catalyzed by **Mo3** as shown in Scheme 7. The amine **1a** interacted with the molybdenum center of catalyst **Mo3** replacing weakly coordinated water molecules with the formation of hydroxo–metal complex **Mo3-I** intermediate. **Mo3-I** undergoes β-hydrogen elimination from the methylene group of benzylamine to the unutilized Mo=O group or Mo–OH group, generating the intermediates **Mo3-II** or **Mo3-II′**, respectively. In this step, the formation of imine, **1a′** occurs which is weakly bound with the metal center. The intermediate complex **Mo3-II** or **Mo3-II′** release the imine producing respective intermediates **Mo3-III** or **Mo3-III′**. In the final step, the intermediate complexes **Mo3-III** or **Mo3-III′** react with $\frac{1}{2}O_2$ to produce the original catalyst **Mo3**. The generated imine coupled with 1,2-diaminobenzene to produce the desired compound 2-substituted benzimidazole, **1c**.

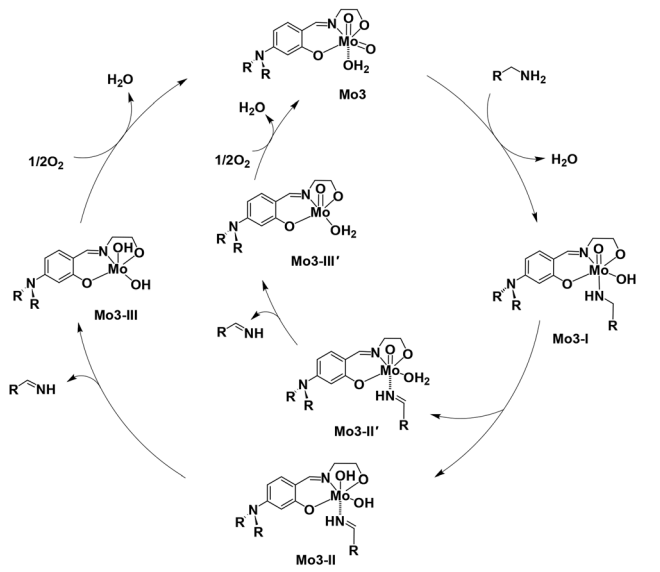

Scheme 7 Proposed mechanism for the oxidation of benzylamine to phenylmethanimine using **Mo3**.

Conclusions

In summary, a new oxomolybdenum-based metallomicellar catalyst, **Mo3** was synthesized, where the coordination entity was connected with two long alkyl chains *via* covalent bonds. The complex **Mo3** was thoroughly characterized using FT-IR, NMR spectroscopy and ESI-MS spectrometry techniques. The micellar aggregation of **Mo3** in water was confirmed through CMC determination and HR-TEM analysis. The double-chain-based catalyst **Mo3** demonstrated superior efficiency in the oxidative synthesis of 2-substituted benzimidazoles from benzylamine in water compared to a similar oxomolybdenum complex with a single alkyl chain in the ligand backbone, **Mo2**. Using the newly developed catalyst **Mo3**, a range of benzimidazole derivatives with different functional groups were synthesized in good to excellent yields in water, utilizing open air as the only oxidant without involving any base or additives. The practical applicability of the developed catalyst was probed by multi-gram scale synthesis and recyclability experiments. Finally, a plausible mechanism was proposed based on some controlled experiments and supporting literature.

Experimental section

Materials and methods

3-Aminophenol, bis(acetylacetonato)dioxomolybdenum(VI), 1-bromohexadecane, bromomethane, 2,4-dihydroxybenzaldehyde were purchased from Sigma-Aldrich. Ethanolamine, $POCl_3$, ^{i}PrOH, and ethyl acetate were purchased from SISCO Research Laboratories Pvt. Ltd, India. The benzylamines **1a–3a**, **6a–8a**, **11a**, **13a**, **15a** and the deuterated solvents were purchased from Sigma-Aldrich, whereas **4a**, **5a** and **16a**, **17a** were purchased from TCI Chemicals (India Pvt. Ltd). Benzylamines **9a**, **10a**, **12a**, **14a** and **19a** were purchased from BLD Chemicals and the 1,2-diaminobenzenes **1b** and **2b** were purchased from Sigma-Aldrich. All the aforementioned purchased chemicals from different sources were used without any further purification.

The NMR spectra were recorded on Bruker Avance-400 and 500 instruments. Fourier Transform Infrared (FT-IR) spectra of the complexes were measured on a model Nexus 670 (FTIR), Centaurms 10× (Microscope) having spectral Range 4000 to 400 cm^{-1} with an MCT-B detector. The ESI-Mass spectrum of the complex was recorded on an Agilent Q-TOF spectrometer in a positive ion mode. HR-TEM images were obtained on HR-TEM, (TecnaiTM G2 TF20) working at an accelerating voltage of 200 kV. The wavelength of the laser used was 632.8 nm with a scattering angle of 90°. LMCM-20 conductivity meter from LABMAN scientific instruments was used for the determination of critical micellar concentration of the complexes. DFT study was performed using the Gaussian 09 software package. The B3LYP (Becke's three-parameter hybrid functional using the LYP correlation) functional was used for geometry optimizations and frequencies with LANL2DZ for the Mo atom, and the 6-31G* basis set for carbon, nitrogen, oxygen and hydrogen. Frequency calculations were performed for the optimized structures to confirm the absence of any imaginary frequencies.

Synthesis of precursor, 3-(dihexadecyl)aminophenol (P_3)

The precursor 3-(dihexadecyl)aminophenol was synthesized following the literature report[36] with necessary modification taking 3-aminophenol and 1-bromohexadecane as starting material. 3-Aminophenol (1.0 g, 9.16 mmol), 1-bromohexadecane (5.59 g, 18.32 mmol) and Na_2CO_3 (1.94 g, 18.32 mmol) were taken in H_2O (10 mL) and ^{i}PrOH (10 mL) solvent mixture. The reaction mixture was allowed to stir for 12 hours under reflux conditions. After completion of the reaction, the solvent was removed under reduced pressure. The obtained crude product was purified by column chromatography using hexane and ethyl acetate as the eluent.

^{1}H NMR (400 MHz, $CDCl_3$, 24 °C): δ 7.05–7.01 (m, 1H), 6.24–6.22 (m, 1H), 6.13–6.09 (m, 2H), 3.23–3.19 (m, 4H), 1.56 (m, 4H), 1.30–126 (m, 52H), 0.90–0.87 (m, 6H) ppm.

$^{13}C\{^1H\}$ NMR (126 MHz, $CDCl_3$, 24 °C): δ 156.85, 149.91, 130.16, 104.84, 102.29, 98.73, 51.31, 32.08, 29.85, 29.78, 29.71, 29.52, 27.40, 27.34, 22.84, 14.27 ppm.

HRMS (ESI) m/z: calculated for $C_{38}H_{71}NO$ + H: 558.5534; found: 558.5609.

Synthesis of precursor, A_3

Aldehyde, A_3 was prepared by the Vilsmeier–Haack method following a literature protocol.[37] Initially, 5.0 mL of dry DMF was cooled to 0–5 °C in an ice bath and $POCl_3$ (0.34 g, 2.24 mmol) was added dropwise into it. The solution was heated at 40 °C for half an hour and a yellow-colored Vilsmeier reagent appeared. The solution was again cooled to 0–5 °C and 3-(hexadecyl)aminophenol (0.5 g, 0.89 mmol) was added dropwise with continuous stirring. The reaction mixture was allowed to stir for 15–20 minutes and heated at 70 °C for 6 hours. After completion of the reaction, the ice-cooled distilled water was added to the reaction mixture. The organic layer was separated from the aqueous layer by phase separation by adding DCM. The organic solvent was evaporated under reduced pressure and the desired product A_3 was purified by column chromatography using hexane and ethyl acetate as eluent.

^{1}H NMR (500 MHz, $CDCl_3$, 24 °C): δ 11.64 (s, 1H), 9.48 (s, 1H), 7.25–7.21 (m, 1H), 6.23–6.21 (m, 1H), 6.03 (s, 1H), 3.31–3.28 (m, 4H), 1.61–1.60 (m, 4H), 1.31–126 (m, 52H), 0.89–0.86 (m, 6H) ppm.

$^{13}C\{^1H\}$ NMR (126 MHz, $CDCl_3$, 24 °C): δ 191.95, 164.44, 154.68, 135.38, 111.51, 104.69, 96.99, 51.38, 32.07, 29.84, 29.80, 29.78, 29.74, 29.71, 29.58, 29.50, 27.43, 27.16, 22.83, 14.25 ppm.

HRMS (ESI) m/z: calculated for $C_{39}H_{71}NO_2$ + H: 586.5485; found: 586.5553.

Synthesis and characterization of ligand, $L_3(H)_2$

The double chain integrated Schiff base ligand $L_3(H)_2$ was synthesized by adopting a literature protocol with necessary modifications.[38] The precursor A_3 (1.0 g, 1.7 mmol) was taken in 15 mL methanol and ethanolamine (0.1 g, 1.7 mmol) was added to the reaction mixture followed by a few drops of acetic acid as a catalyst. The reaction mixture was stirred for 3 h under reflux conditions. After completion of the reaction the obtained clear solution was allowed to stand overnight to obtain a yellow crystalline solid Schiff base compound.

^{1}H NMR (400 MHz, $CDCl_3$, 24 °C): δ 8.05 (s, 1H), 6.99–6.97 (m, 1H), 6.13–6.11 (m, 1H), 6.05 (s, 1H), 3.86–3.84 (m, 2H), 3.64–3.63 (m, 2H), 3.27–3.24 (m, 4H), 1.58 (m, 4H), 1.30–126 (m, 52H), 0.89–0.86 (m, 6H) ppm.

$^{13}C\{^1H\}$ NMR (126 MHz, $CDCl_3$, 24 °C): δ 167.67, 164.48, 152.74, 133.36, 108.23, 103.59, 98.70, 62.44, 59.02, 51.19, 32.07, 29.84, 29.80, 29.75, 29.66, 29.50, 27.60, 27.25, 22.83, 14.26 ppm.

HRMS (ESI) m/z: calculated for $C_{41}H_{76}N_2O_2$ + H: 629.5907; found: 629.5974.

Synthesis of double chain based oxomolybdenum complex Mo3

The oxomolybdenum complex $[MoO_2(L_3)(H_2O)]$, **Mo3** was synthesized following a general method demonstrated in our earlier report.[13] The ligand $L_3(H)_2$ (0.5 g, 0.8 mmol) and bis(acetylacetonato)dioxomolybdenum(VI) (0.26 g, 0.8 mmol) were dissolved in 15 mL methanol and stirred for 3 h under reflux conditions. After completion of the reaction the obtained yellow colored solution was allowed to stand overnight. A yellow-colored semi-crystalline was observed, which was filtered and dried under vacuum. The obtained yellow solid was taken in 15 mL water and stirred for 1 hour at room temperature. The precipitate was further filtered and dried under a vacuum, providing the desired compound **Mo3**.

^{1}H NMR (500 MHz, $CDCl_3$, 24 °C): δ 8.31 (s, 1H), 7.16–7.14 (m, 1H), 6.31–6.29 (m, 1H), 6.19 (s, 1H), 4.63–4.60 (m, 2H), 4.16–4.13 (m, 2H), 3.31–3.28 (m, 4H), 1.31–1.26 (m, 56H), 0.89–0.86 (m, 6H) ppm.

$^{13}C\{^1H\}$ NMR (126 MHz, $CDCl_3$, 24 °C): δ 164.09, 163.48, 155.45, 134.97, 109.82, 106.58, 99.88, 71.24, 63.72, 51.50, 32.07, 29.89, 29.85, 29.81, 29.74, 29.61, 29.50, 27.54, 27.20, 22.83, 14.25 ppm.

IR (KBr pellet) ν = 2917, 2856, 1607, 1523, 1461, 1233, 931, 897, 636 cm^{-1}.

MS (ESI) *m*/*z*: calculated for $[(\mathbf{Mo3} + H) - H_2O]^+$: 757.4786; found: 757.4768.

General procedure for the oxidative coupling reactions

A mixture of benzylamine (0.9 mmol), 1,2-diaminobenzene (0.75 mmol) and **Mo3** (1.5 mol%) was taken in 0.5 mL water in a ~12.0 mL reaction tube (~5.0 × 2.0 cm of height × width) fitted with a reflux condenser. The reaction mixture was stirred for 18 h at 80 °C temperature under open air atmosphere. The progress of the reaction was monitored by TLC. After completion of the reaction, 0.5 mL water was added to the reaction mixture, and the aqueous layer was extracted with ethyl acetate (3 × 1 mL). The organic layer containing benzimidazole was dried over anhydrous sodium sulfate and evaporated under reduced pressure. The desired product was purified by column chromatography (silica gel) using hexane–ethyl acetate as an eluent. The purified product was characterized by ^{1}H and ^{13}C NMR spectroscopy.

Author contributions

D. K. C., P. S. and P. T. designed the project. P. S. and P. T. were involved in the synthesis of surfactant-based ligands, molybdenum complexes, and their characterization. P. S. carried out the experiments related to catalysis. P. T. was involved in scientific discussions with P. S. on a regular basis. The manuscript was written by all authors. D. K. C. is the principal investigator and managed the project.

Data availability

The data supporting this article have been included as part of the ESI.‡

Conflicts of interest

There are no conflicts to declare.

Acknowledgements

D. K. C. acknowledges financial support provided by IIT Madras under an Exploratory Research Project (RF20210651CYRFER008112). We thank the Department of Chemistry, IIT Madras for the instrumentation facilities.

References

1 T. Dwars, E. Paetzold and G. Oehme, *Angew. Chem., Int. Ed.*, 2005, **44**, 7174–7199.
2 C.-J. Li and L. Chen, *Chem. Soc. Rev.*, 2006, **35**, 68–82.
3 G. L. Sorella, G. Strukul and A. Scarso, *Green Chem.*, 2015, **17**, 644–683.
4 T. Kitanosono, K. Masuda, P. Xu and S. Kobayashi, *Chem. Rev.*, 2018, **118**, 679–746.
5 S. Kobayashi and K. Manabe, *Acc. Chem. Res.*, 2002, **35**, 209–217.
6 J. Zhang, X. G. Meng, X. C. Zeng and X. Q. Yu, *Coord. Chem. Rev.*, 2009, **253**, 2166–2177.
7 J. Li, Y. Tang, Q. Wang, X. Li, L. Cun, X. Zhang, J. Zhu, L. Li and J. Deng, *J. Am. Chem. Soc.*, 2012, **134**, 18522–18525.
8 J. E. W. Cull, A. Richard and J. Scott, *Green Chem.*, 2013, **15**, 362–364.
9 X. Liang, Y. Gui, K. Li, J. Li, Z. Zha, L. Shi and Z. Wang, *Chem. Commun.*, 2020, **56**, 11118–11121.
10 R. D. Chakravarthy, V. Ramkumar and D. K. Chand, *Green Chem.*, 2014, **16**, 2190–2196.
11 P. Thiruvengetam, R. D. Chakravarthy and D. K. Chand, *J. Catal.*, 2019, **376**, 123–133.
12 P. Thiruvengetam and D. K. Chand, *J. Org. Chem.*, 2022, **87**, 4061–4077.
13 P. Thiruvengetam, P. Sunani and D. K. Chand, *ChemSusChem*, 2024, **17**, e202301754.
14 J. K. Virdi, A. Dusunge and S. Handa, *JACS Au*, 2024, **4**, 301–317.
15 T. Lorenzetto, D. Frigatti, F. Fabris and A. Scarso, *Adv. Synth. Catal.*, 2022, **364**, 1776–1797.
16 L. Onel and N. J. Buurma, *Annu. Rep. Prog. Chem., Sect. B*, 2010, **106**, 344–375.
17 P. C. Griffiths, I. A. Fallis, T. Chuenpratoom and R. Watanesk, *Adv. Colloid Interface Sci.*, 2006, **122**, 107–117.
18 Q. Gao, Y. Liu, S.-M. Lu, J. Li and C. Li, *Green Chem.*, 2011, **13**, 1983–1985.
19 T. Rispens and J. B. F. N. Engberts, *Org. Lett.*, 2001, **3**, 941–943.
20 A. P. H. J. Schenning, J. H. Lutje Spelberg, D. H. W. Hubert, M. C. Feiters and R. J. M. Nolte, *Chem. – Eur. J.*, 1998, **4**, 871–880.
21 J. Li, Z. Lin, Q. Huang, Q. Wang, L. Tang, J. Zhu and J. Deng, *Green Chem.*, 2017, **19**, 5367–5370.
22 T. Lorenzetto, F. Fabris and A. Scarso, *Curr. Opin. Colloid Interface Sci.*, 2023, **64**, 101689.
23 M. Amini, M. M. Haghdoost and M. Bagherzadeh, *Coord. Chem. Rev.*, 2013, **257**, 1093–1121.
24 S. C. A. Sousa and A. C. Fernandes, *Coord. Chem. Rev.*, 2015, **284**, 67–92.
25 P. Thiruvengetam and D. K. Chand, *J. Indian Chem. Soc.*, 2018, **95**, 781–788.
26 O. O. Ajani, D. V. Aderohunmu, S. J. Olorunshola, C. O. Ikpo and I. O. Olanrewaju, *Orient. J. Chem.*, 2016, **32**, 109–120.
27 Y. Bansal and O. Silakari, *Bioorg. Med. Chem.*, 2012, **20**, 6208–6236.
28 D. I. Shah, M. Sharma, Y. Bansal, G. Bansal and M. Singh, *Eur. J. Med. Chem.*, 2008, **43**, 1808–1812.
29 S. A. Galal, K. H. Hegab, A. S. Kassab, M. L. Rodriguez, S. M. Kerwin, A.-M. A. El-Khamry and H. I. El Diwani, *Eur. J. Med. Chem.*, 2009, **44**, 1500–1508.
30 K. M. H. Nguyen and M. Largeron, *Chem. – Eur. J.*, 2015, **21**, 12606–12610.
31 K. Gopalaiah and S. N. Chandrudu, *RSC Adv.*, 2015, **5**, 5015–5023.
32 K. M. H. Nguyen and M. Largeron, *Eur. J. Org. Chem.*, 2016, 1025–1032.

33 C. Weerakkody, D. Rathnayake, J. He, B. Dutta, P. Kerns, L. Achola and S. L. Suib, *ChemCatChem*, 2019, **11**, 528–537.
34 K. Bano, D. A. Kisan and T. K. Panda, *Eur. J. Inorg. Chem.*, 2022, e202200023.
35 M. Kocsis, M. Szabados, S. B. Ötvös, G. F. Samu, Z. Fogarassy, B. Pécz, Á. Kukovecz, Z. Kónya, P. Sipos, I. Pálinkó and G. Varga, *J. Catal.*, 2022, **414**, 163–178.
36 J. F. Ge, C. Arai, M. Kaiser, S. Wittlin, R. Brun and M. Ihara, *J. Med. Chem.*, 2008, **51**, 3654–3658.
37 R. Nazir, P. Danilevicius, A. I. Ciuciu, M. Chatzinikolaidou, D. Gray, L. Flamigni, M. Farsari and D. T. Gryko, *Chem. Mater.*, 2014, **26**, 3175–3184.
38 C. R. Bhattacharjee, C. Datta, G. Das and P. Mondal, *Liq. Cryst.*, 2012, **39**, 639–646.
39 O. A. Rajan and A. Chakravorty, *Inorg. Chem.*, 1981, **20**, 660–664.
40 Y. Maeda, N. Kakiuchi, S. Matsumura, T. Nishimura, T. Kawamura and S. Uemura, *J. Org. Chem.*, 2002, **67**, 6718–6724.